Bulg. J. Phys. **42** (2015) 372–381

Nuclear Physics Studies at ELI-NP

D.L. Balabanski and the ELI-NP Science Team
ELI-NP, Horia Hulubei National Institute for R&D in Physics and Nuclear Engineering (IFIN-HH), 077125 Magurele, Romania

Abstract. The mission of the Extreme Light Infrastructure – Nuclear Physics (ELI-NP) facility is to use extreme electromagnetic fields for nuclear physics research. At ELI-NP, high-power lasers together with a very brilliant γ-ray beam are the main research tools. Their targeted operational parameters are described. The emerging experimental program of the facility in the field of nuclear physics is reported and the main directions of the research envisioned are presented. The experimental instrumentation, which will operate at ELI-NP for the realization of the research program, is discussed. The expected impact of ELI-NP on the future advance of the field is summarized.

PACS codes: 07.85.Fv, 29.20.Ej, 25.20.-x

1 Introduction

The Extreme Light Infrastructure (ELI) Pan-European facility initiative represents a major step forward in quest for achieving extreme electromagnetic fields. The Extreme Light Infrastructure – Nuclear Physics (ELI-NP) is one of the three pillars of ELI, and is under construction in Magurele, Romania. It is designed as a state-of-the-art laboratory for nuclear physics research and applications with extreme electromagnetic fields and will host a high-power laser system (HPLS) consiting of two 10 PW lasers and a brilliant γ-beam system (GBS). The facility can provide simultaneously two synchronized high-power laser beams on the target [1]. The HPLS has six output lines, two of 10 PW, two at 1 PW and two at 100 TW. The GBS is superior to existing facilities in terms of γ-ray intensity and resolution. At ELI-NP the HPLS and the GBS will be synchronized and experiments which combine an intense laser beam with a brilliant γ beam will be possible. The mission of the laboratory is to cross the frontiers of known laser-driven and γ-beam nuclear physics. In particular, due to the laser intensities of the order of 10^{23} W/cm^2 at the target, a wide range of laser-driven accelerated heavy-ion beams will be produced, and because of the brilliant, narrow-bandwidth, highly polarized γ beams, reaching spectral densities of the order of 10^4 photons/(eV·cm^2), precise photonuclear measurements in the energy range between 200 keV and 19.5 MeV will be done. Different types of experiments, using either the HPLS, or the GBS, or both of them, are considered [2–5]. They

are described in detail in a number of technical design reports (TDR) [6],which were approved for implementation in 2015.

2 Laser-Driven Experiments

Laser-driven plasma-based particle acceleration was proposed by Tajima and Dawson [7]. Today, laser plasma acceleration (LPA) studies are a flourishing research field with ongoing experimental programs worldwide. Much of this growth is due to the rapid development of the chirped-pulse amplification (CPA) laser technology, pioneered by Strickland and Mourou [8].

High-power laser-matter interactions produce a wake of plasma oscillations, which are due to localized volumes of low and high densities of electrons. As a result, the electrons not only oscillate at the frequency of the field, but are also accelerated in direction of the wake field. Exploring this mechanism, electron beams up to GeV energies have been realized with pC charges per laser pulse having an energy spread of 1-2% and an emitance of 10^5 mm·mrad. For a recent review see *e.g.* Ref. [9].

Next, protons and heavy-ions were accelerated. Two major acceleration mechanisms have been identified, target normal sheath acceleration (TNSA) [10] and radiation pressure acceleration (RPA) [11]. In TNSA, the acceleration of the ions is due to the strong field set up by a sheath of laser-accelerated electrons, which are pushed by the laser electromagnetic field to the rear side of a solid target, establishing by charge separation an electrostatic field with a large enough gradient to drag the ions. The RPA mechanism is driven directly by the radiation pressure exerted by super-intense laser pulses on overdense plasmas. As a result, the electrons are driven out of the target foil via light pressure, which in turn leads to acceleration of the ions in the resulting dipolar field. In the TNSA regime, the proton energy E_p scales scales with the laser intensity I_L, as $E_p \sim \sqrt{I_L}$, while in the RPA regime it scales as $E_p \sim I_L$.

Note that the progress in the field of LPA and the present state-of-the-art results are obtained with lasers with intensities up to 1 PW. For example, in a recent experiment at ELFIE, the 100 TW laser facility at LULI, Palaiseau, Negoita *et al.* demonstrated the feasibility of *in situ* measurement of short-lived isomers with lifetimes down to millisecond [12]. A target for proton acceleration, a 25 μm Al foil replaced after each shot, was placed in the laser focus, and an activation target, a 50 μm ^{nat}Zr foil, was mounted 4 cm downstream along the proton-beam axis. Excited states in ^{90}Nb were populated in the ^{90}Zr(p, n) reaction. The decay of the 382-keV ($T_{1/2} = 6.19(8)$ ms), 124.7-keV ($T_{1/2} = 18.81(6)$ s), and 122.4-keV ($T_{1/2} = 63(2)$ μs) isomers in ^{90}Nd was observed in the experiment. Note that the μs 122.4-keV isomer is fed by the 124.7-keV isomer. The γ rays of interest were detected with a 1.5" $\times$ 1.5" $LaBr_3$:Ce crystal, coupled to a gated preamplifier. About 10^2 counts per laser shot have been measured for each iso-

meric transition. Taking into account the detector efficiency, it was concluded that about 10^6 isomers were produced per laser shot.

The HPLS of ELI-NP will provide much higher laser intensities and will further contribute to the understanding of the LPA mechanism. The experiments will aim at the production of heavy-ion beams, including actinide beams. The ultimate goal of this program is to explore the suggested fission-fusion mechanism [13]. In this reaction laser-accelerated actinide beam with very high intensity, exceeding classical accelerator beams by 10-15 orders of magnitude, impinge on an actinide target. As a result, beam- and target-like ions fission, creating a jet with a high temperature and high density of neutron-rich fission fragments. In its volume, subsequent fission might occur, resulting in very neutron-rich isotopes. For example, the fusion of the light fragments,

$$^{A_1}_{N_1}F_{Z_1} + ^{A_2}_{N_2}F_{Z_2} = ^{<192>}_{<118>}X_{<74>} - xn, \tag{1}$$

will produce isotopes in the vicinity of the *r*-process $N = 126$ waiting point. The successful performance of such experiments requires mastering of the heavy-ion LPA techniques, which are at present in their infancy. The success of the experiments relies on further development of the mass-separation techniques, designing devices, that can handle beams of reaction products with intensities which are far beyond the beams which are delivered by classical accelerators. A key instrument for the success of this experimental program will be the design and the construction of a large-acceptance fragment separator.

3 Experiments with Brilliant γ Beams

The ELI-NP GBS will deliver highly-polarized ($\geq$95%) tunable γ beams of spectral density of 10^4 photons/(s·eV) in the range from 200 keV to 19.5 MeV with a bandwidth of $\geq$0.3%, and a source spot size smaller than 30 μm [14, 15]. The peak brilliance of the γ-ray beam is expected to be larger than 10^{20} photons/(sec·mm^2·mrad^2·0.1%). The γ beams will be produced through laser Compton backscattering (LCB) off an accelerated electron beam delivered by a linear accelerator. In the LCB process maximum up-shift is achieved in head-on collisions. The laser beam interacts with the electron beam at a small angle, θ_L, and the energy of the scattered γ rays at angle θ_γ, $E_\gamma(\theta_\gamma)$, (see Figure 1) is

$$E_\gamma(\theta_\gamma) = 2\gamma_e \cdot \frac{1+\cos\theta_L}{1+(\gamma_e\theta_\gamma)^2 + \dfrac{4\gamma_e E_L}{m_e c^2}} \cdot E_L, \tag{2}$$

where $\gamma_e = \sqrt{1-(v_e/c)^2}$, v_e is the electron velocity, m_e is the rest mass of the electron, and c is the speed of light. For a green-light laser, $E_L = 2.3$ eV (515 nm), backscattering off 720-MeV electrons yields γ rays with $E_\gamma < 20$ MeV.

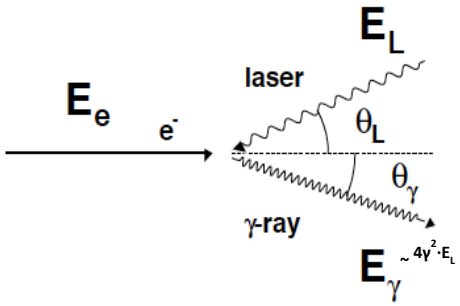

Figure 1. Geometry of the inverse Compton scattering of a laser photon with energy E_L incident at an angle θ_L with respect to the axis of the relativistic electron beam. The photon is scattered at angle θ_γ with respect to the electron beam.

The low cross section of the process ($\sigma_{LCB} \approx 10^{-25}$ cm^2) needs to be compensated by high photon and electron densities at the interaction point.

For the ELI-NP GBS Yb:YAG J-class laser system was adopted, delivering high quality $M^2 < 1.2$ picosecond (3.5 ps FWHM) laser pulses that are focused down to focal spot sizes of about 30 μm at the collision points. The laser pulse repetition rate is 100 ± 5 Hz. The electron bunches are delivered by a high-brightness electron Linac. It runs at a repetition rate of 100 Hz, synchronized with Yb:YAG laser, injecting from the photo-injector into the booster Linac trains of 32 bunches separated by 16 ns over a 512 ns flat RF pulse.

3.1 Nuclear resonance fluorescence experiments

The γ beam brilliance and bandwidth at ELI-NP will increase the sensitivity of nuclear resonance fluorescence (NRF) experiments, which allows to perform such experiments on small target samples. In this way, materials which are available in quantities of few milligrams, *e.g.* actinide isotopes, can be studied. The NRF program at ELI-NP will focus on studies of the low-lying dipole strength, such as the scissors mode, and the fragmentation of the strength of soft modes, such as the pigmy dipole resonance (PDR). The brilliance of the γ beam will enable $\gamma\gamma$-coincidence experiments, which provides the opportunity for detailed investigation of the decay of photo-excited states. All these studies will benefit from the high polarization of the γ beam, which allows to distinguish $M1$ from $E1$ transitions. In order to carry out these experiments, a multi-detector array ELIADE, consisting of eight large TIGRESS-type segmented Clover HPGe detectors [16], is under construction at ELI-NP [6]. The detectors will be mounted in two rings at 98° and 135° with respect of the γ beam, reaching a γ-ray detection efficiency of about 6%. Large-volume $LaBr_3$:Ce detectors might be also added to the set-up.

3.2 Experiments above the neutron evaporation threshold

Experiments above the neutron separation threshold, S_n, will be performed alongside NRF studies for a complete investigation of the nuclear photo-absorption process and decay modes. Energy and angular differential photonuclear reaction cross-sections and elastic (γ,γ) and inelastic (γ,γ') scattering will be studied within this research program. The observation of the energy and angular distribution of neutron and γ decays of the photon-excited giant resonance states in stable and unstable nuclei provide valuable information about the neutron-γ decay branching ratios, (γ, xn), (γ,γ) and (γ,γ') cross sections and absolute transition strengths, the multipolarity of the reaction neutrons, the multipole mixing ratios of the γ transitions and the spins and parities of the excited states. Experimental data on (γ,γ) and (γ,γ') reactions above S_n are scarce because of their low cross sections and the difficulty for precise determination of the excitation and decay energy. The unique intensity, energy resolution and polarization of the ELI-NP γ-beam will make such measurements possible. In order to carry out these experiments, a multi-detector array, ELIGANT-NT, consisting of 30 large 3" $\times$ 3" $LaBr_3$:Ce and $CeBr_3$ detectors, arranged in rings at backward angles, and 30 liquid scintillators is under construction at ELI-NP [6]. For photoneutron cross-section experiments another array, ELIGANT-N, consisting of 30 ^{3}He counters is being assembled [6]. This experimental program includes also studies of (γ,n) cross sections of the ^{138}La$(\gamma, n)^{137}$La and ^{180m}Ta$(\gamma, n)^{179}$Ta reactions, which are of key importance for the understanding of the *p*-process and provide constraints on the explosive dynamics of massive stars.

3.3 Charge-particle experiments

The principle of detailed balance allows the determination of the cross section of an (α, γ) process from the measurement of the time inverse (γ, α) reaction with γ-ray beams. Studying reactions by means of inverse photo-disintegration has the advantage of having different systematic uncertainties than those of charge-particle induced reactions measured at low energies of astrophysics interest. Several key nuclear astrophysics reactions were identified to be studied at ELI-NP [6]. These include the ^{12}C$(\alpha, \gamma)^{16}$O reaction at the Gamow peak (300 keV), which is related to the carbon-to-oxygen ratio at the end of the He burning, one of the key open questions of nuclear astrophysics [17]. Other proposed studies include the ^{24}Mg$(\gamma, \alpha)^{20}$Ne reaction, which governs the downward flow from ^{24}Mg to ^{4}He. The ^{22}Ne$(\gamma, \alpha)^{18}$O reaction, which is related to the production of ^{22}Ne, which provides one of the neutron sources for s-process nucleosynthesis in massive stars through the ^{22}Ne(α, n) reaction. The ^{19}F$(\gamma, p)^{18}$O reaction, which is a measure for the loss of catalytic materials from the CNO cycle, providing at the same time a link to the NeNa cycle. The ^{21}Ne$(\gamma, \alpha)^{17}$O reaction will allow the determination of the cross section at lower energies of

the time-reversal ^{17}O$(\alpha,\gamma)^{21}$Ne reaction, which is essential for determining the role of ^{16}O as a neutron poison in the CNO cycle. These experiments will benefit from two instruments, which are currently being designed for ELI-NP, a time-projection chamber with electronic read-out based on the GEM technology [18], ELI-eTPC, which is being built in collaboration with the Warsaw University [6], and a 4π double-sided Si strip array, ELISSA, which is designed together with the INFN LNS [6].

3.4 Photofission experiments

Photofission measurements enable selective investigation of extremely deformed nuclear states in the light actinides and can be utilized to better understand the landscape of the multiple-humped potential energy surface (PES) in these nuclei. The experimental approach to investigate extremely deformed collective and single particle nuclear states of the light actinides is based on the observation of transmission resonances in the prompt fission cross section [19, 20]. Observing transmission resonances as a function of the excitation energy caused by resonant tunneling through excited states in the 3^{rd} minimum of the potential barrier, allows us to identify the excitation energies of the hyperdeformed (HD) states. The selectivity of these measurements originates from the low and reasonably well-defined amount of angular momentum transferred during the photo-absorption process. High-resolution studies can be performed on the mass, atomic number, and kinetic energy distributions of the fission fragments following the decay of well-defined initial states in the first, second and third minima of the PES in the region of the light actinides. Experiments, which have been carried out at the HIγS γ-beam facility at Duke University, although with low resolution, indicate the existence of a 3^{rd} PES minimum [21].

These studies call for developments of state-of-the-art fission detectors to exploit the unprecedented properties of the high-flux, Compton backscattered γ beams having a very small, millimeter beam spot size [6]. A multi-target detector array, ELITGEM, is under development in collaboration with MTA Atomki, consisting of position sensitive gas detector modules based on the state-of-the-art THGEM technology [22]. The foreseen millimeter γ beam-spot size allows to develop considerably more compact photofission detectors than those of before. In addition, the well-focused γ beam also defines a distinct fission position, so a remarkably improved angular resolution can be achieved.

For the measurement of the mass and atomic number distribution of the fission fragments a highly-efficient, five-folded, Frisch-gridded twin ionization chamber [23], which will be used as Bragg ionization chamber (BIC) [24], is under development in collaboration with MTA Atomki. The twin ionization chamber will be equipped with double-sided Si strip detectors for measurements of light particle or α emission probability from the highly-deformed compound state and to detect any ternary particles from fission. Atomic numbers will be extracted by tracking and digitizing the Bragg curve of the ions.

3.5 The IGISOL facility at ELI-NP

The GBS γ-ray beam will cover selectively energy region of the giant dipole resonance (GDR) of the fissile target, which makes it an ideal tool to induce photo-fission of the target nuclei. An IGISOL facility at ELI-NP [6] is been designed in collaboration with the GSI and the University of Giessen, Germany. The IGISOL technique [25] allows the extraction of the isotopes of refractory elements, which do not come out from standard ISOL targets. It will consist of a cryogenic stopping cell (CSC) [26], where photofission fragments will be produced in Uranium targets, coupled to a radiofrequency quadrupole (RFQ) beam line that extracts, cools, separates on mass and bunches the ions from the CSC and a multiple-reflection time-of-flight mass separator (MR-ToF-MS). The combined mass resolving power of the whole beam line will exceed $3 \cdot 10^5$ [6], which allows isomer $vs.$ ground state separation.

Extensive series of simulations have been carried out for determination of the expected fission rates and the extraction efficiency of the IGISOL CSC. Two independent implementations of the photofission process were developed within the Geant4 framework [27]. Both use (γ,f) cross-section parameterizations for various actinides from Ref. [28]. In the first implementation, we derived our own concrete class G4PhotoFission, which inherited from the Geant4 base class G4HadronInelastic, to generate final state for photo-fission and process used to handle photon-induced fission is G4ParaFissionModel [29,30]. The information about the secondaries and their related distributions could be retrieved by accessing appropriately to G4SteppingManager [29]. The second implementation defines the final state distributions from existing photofission measurements, the first fragment proton and neutron number (Z, N) distribution is taken from that measured in photofissions from ultra-peripheral ^{238}U($\gamma^{\star}$,f)^{208}Pb collisions [31], with the virtual energy below 25 MeV. Since these measurements were done up to $Z = 52$, an extrapolation based on Gaussian fits is used for higher Z isotopes [30]. Considering a stack of target foils of 800 mg total thickness placed in a gas cell, which are irradiated by a γ beam of $5 \cdot 10^{10}$ γ/s in the 10-18.5 MeV energy range, the fission rate is 10^7 fission/s [30].

Next, fragment release efficiency from the targets was evaluated using several ion charge state paramerizations [32–35] for calculation of stopping powers. The results from the calculations were compared to measurements of ionic charge-state distributions produced in thermal neutron-induced fission of ^{235}U [36]. In this way, the target release efficiency was found to be 10-20% depending on the target thickness. Finally, the ion stopping in a CSC was evaluated [37]. A CSC with two stage longitudinal extraction using a combination of DC and RF fields was considered. Such a gas cell combines fast extraction times of about 5 ms and high extraction efficiency of 50% [38]. The geometry of the target stack in the CSC was optimized with respect to the number of targets, the foil tickness, the tilt angle with respect to the beam and the distance between the foils [37].

The ion-release rate from the target assembly for an optimal configuration, taking into account the available space for the ELI-NP IGISOL demonstrator [6] at the high-energy γ beam line, is $1.3(2)\cdot 10^6$ ions/s [37]. In this case about 220 mg ^{238}U material will be used, which exhausts only about 10% of the available γ beam. The ion stopping in the gas cell for different gas densities and temperatures was studied, too, which allows to define its dimensions. Thus, if the CSC operates at 300 mbar and 70 K, the diameter of the inner chamber is $\varnothing = 25$ cm and its length is $L = 150$ cm. Possible space-charge effects, which might result from the ionic currents in the CSC at these ion rates, were evaluated and was demonstrated that only 2% of the fragments that are slowed down to around 2 keV remain in the high-value space-charge region can no longer be drifted out of it by the DC field [37].

In short, an IGISOL facility at ELI-NP will produce competitive number of rare isotopes of refractory elements compared to other facilities worldwide.

3.6 Nuclear physics applications

Different applied research problems will be studied at ELI-NP, both with high-power laser beams and brilliant γ beams. These include material modification at extreme electromagnetic fields, γ imaging, development of γ-analytical techniques for material research and cultural heritage studies, and production of new radioisotopes for medical research [6].

4 Combined Laser-Gamma Experiments

ELI-NP may become the first research laboratory where stellar photoreactions are induced and detected. At ELI-NP an experimental program, aiming at inducing stellar photoreactions by producing isomers with the high-power lasers and photo-exciting them with the brilliant γ-ray beam, is proposed [6].

Laser-acceleration of electrons with kinetic energies of the order of MeV followed by the subsequent production of Bremsstrahlung radiation most effectively produces isomers. Isomeric states are populated either in the inelastic electron scattering, or in a photoabsorption reactions. Photoabsorption excites a nucleus in either bound, or unbound states. The bound states decay to the isomeric state via γ-decay [39], while the unbound states undergo neutron emission followed by γ-decay to the isomeric state [40]. Therefore, a key first step in this experimental program, is the production a vast number of MeV electrons by laser-driven acceleration. An optimization of the operation conditions of the fs pulse-width lasers will be done. In this first stage of the experimental program, isomeric γ-decay will be observed, using the technique described in above for measurement of the γ-decay of isomeric states in laser-driven (p, n) reactions [12].

In the second stage of the experimental program, the production of sufficient number of long-lived isomers per laser shot will be followed by subsequent synchronized irradiation with a γ-ray beam, in order to photo-excite them. Photoexcitation of isomers will be verified by detecting photoneutrons. The signal-to-noise ratio, which is limited by the fact that a relatively small number of isomers are produced by a single laser shot, can be improved by applying a proper time gate for the synchronized irradiation of the laser and γ-ray beams. A study of the $I^{\pi} = 11/2^{-}, T_{1/2} = 32$ ms 121-keV isomer in ^{155}Gd is considered as a day-one experiment. The produced isomers will be photo-excited just above the neutron threshold at 6635 keV by a highly monochromatic γ beam with an energy spread 0.5% (33 keV) in FWHM at energies between 6514 and 6635 keV. Thus, photoneutron emission in ^{155}Gd will occur selectively from the isomeric state. For the neutron detection, the detector arrays, which are designed for experiments above the neutron-evaporation threshold [6], can be used.

5 Conclusions

The ELI-NP facility combines two major research instruments with beyond state-of-the-art performance, a HPLS and a GBS which are nowadays under construction. The HPLS will deliver every minute light pulses with intensity 10^{23} W/cm^2. The GBS will deliver tunable, brilliant, narrow-bandwidth γ beams with energies up to 20 MeV. The superior parameters of the basic equipment of the new laboratory has been used to define a research program, which addresses key questions of modern nuclear physics and will allow the exploration of new frontiers in science. For the realization of the scientific program at ELI-NP, a large number of detector systems have been suggested and designed by the different TDR working groups [6], and are now under construction. A large scientific community from all over the globe has been involved and participates in this endeavour. Today ELI-NP is on schedule and is expected to be commissioned and to start operations as an open-access facility in 2018.

Acknowledgements

This work is supported by Extreme Light Infrastructure — Nuclear Physics (ELI-NP) -– Phase I, a project co-financed by the European Union through the European Regional Development Fund.

References

[1] N.V. Zamfir (2015) *Nucl. Phys. News* **25:3** 34.

[2] *ELI-NP White Book* (2010) `http://www.eli-np.ro/documents/ELI-NP-WhiteBook.pdf`

[3] D. Ursescu *et al.* (2013) *Proc. SPIE* **8780** 87801H.

[4] N.V. Zamfir (2014) *EPJ Web of Conferences* **66** 11043.
[5] D.L. Balabanski *et al.* (2014) *EPJ Web of Conferences* **78** 06001.
[6] ELI-NP TDR teams (2015) *Rom. Rep. Phys.* (in print).
[7] T. Tajima and J.M. Dawson (1979) *Phys. Rev. Lett.* **43** 267.
[8] D. Strickland and G. Mourou (1985) *Opt. Commun.* **56** 219.
[9] E. Esarey, C.B. Schroeder and W.P. Leemans (2009) *Rev. Mod. Phys.* **81** 1229.
[10] S. Wilks *et al.* (2001) *Phys. Plasmas* **8** 542.
[11] T. Esirkepov *et al.* (2004) *Phys. Rev. Lett.* **92** 175003.
[12] F. Negoita *et al.* (2015) *AIP Conf. Proc.* **1645** 228.
[13] D. Habs *et al.* (2011) *Appl. Phys. B* **103** 741.
[14] O. Adriani *et al.* (2014) arXiv:1407.3669 [physics.acc-ph]
[15] C.A. Ur *et al.* (2015) *Nucl. Instr. and Meth. B* **355** 198.
[16] C.E. Svensson *et al.* (2005) *Nucl. Instr. Meth. A* **540** 348.
[17] W.A. Fowler (1984) *Rev. Mod. Phys.* **56** 149.
[18] F. Sauli (1998) *Nucl. Instr. and Meth. A* **386** 531.
[19] P.G. Thirolf and D. Habs (2002) *Prog. Part. Nucl. Phys.* **49** 352.
[20] A. Krasznahorkay (2011) in *Basics of Nuclear Science*, Handbook of Nuclear Chemistry, vol. 1, eds. A. Vertes *et al.*; Springer, Berlin, p. 281.
[21] L. Csige *et al.* (2013) *Phys. Rev. C* **87** 044321.
[22] C.K. Shalem *et al.* (2006) *Nucl. Inst. and Meth. A* **558** 468.
[23] C. Budtz-Jorgensen *et al.* (1987) *Nucl. Instr. Meth. A* **258** 209.
[24] W. Neubert (1985) *Nucl. Instr. Meth. A* **237** 535.
[25] J. Aysto *et al.* (1992) *Phys. Rev. Lett.* **69** 1167.
[26] M. Ranjan *et al.* (2015) *Nucl. Inst. and Meth. A* **770** 87.
[27] S. Agostinelli *et al.* (2013) *Nucl. Inst. and Meth. A* **506** 250.
[28] J.T. Caldwell *et al.*, *Phys. Rev. C* **21** 1215.
[29] P.V. Cuong (2009) *Development of a new surface ion-source and ion guide in the ALTO project*, PhD Thesis, Univ. Paris-Sud, Orsay.
[30] P. Constantin, D.L. Balabanski, and P.V. Cuong (2015) *Nucl. Inst. and Meth B* (in print).
[31] C. Donzaud *et al.* (1998) *Eur. Phys. J. A* **1** 407.
[32] J.F. Ziegler and J.M. Manoyan (1988) *Nucl. Inst. and Meth. B* **35** 215.
[33] J.F. Ziegler, J.P. Biersack, U. Littmark (1985) *The Stopping and Range of Ions in Matter, vol. 1*, Pergamon Press, Oxford.
[34] K. Shima *et al.* (1982) *Nucl. Inst. and Meth.* **200** 605.
[35] G. Schiwietz and P.L. Grande (2001) *Nucl. Inst. and Meth. B* **175-177** 125.
[36] H. Wohlfarth *et al.* (1978) *Z. Phys. A* **287** 153.
[37] P. Constantin, D.L. Balabanski, and P.V. Cuong (2015) *Nucl. Inst. and Meth B* (submitted).
[38] T. Dickel *et al.* (2014) *GSI Report* GSI-SR2013-NUSTAR-FRS-09, p. 106.
[39] D. Belic *et al.* (1999) *Phys. Rev. Lett.* **83** 5242.
[40] S. Goko *et al.* (2006) *Phys. Rev. Lett.* **96** 192501.